A TEMPERATURE GRADIENT METHOD FOR LIPID PHASE DIAGRAM CONSTRUCTION USING TIME-RESOLVED X-RAY DIFFRACTION

MARTIN CAFFREY AND FREDERICK S. HING
Section of Biochemistry, Molecular and Cell Biology, Cornell University, Ithaca, New York 14853

ABSTRACT A method that enables temperature-composition phase diagram construction at unprecedented rates is described and evaluated. The method involves establishing a known temperature gradient along the length of a metal rod. Samples of different compositions contained in long, thin-walled capillaries are positioned lengthwise on the rod and "equilibrated" such that the temperature gradient is communicated into the sample. The sample is then moved through a focused, monochromatic synchroton-derived x-ray beam and the image-intensified diffraction pattern from the sample is recorded on videotape continuously in live-time as a function of position and, thus, temperature. The temperature at which the diffraction pattern changes corresponds to a phase boundary, and the phase(s) existing (coexisting) on either side of the boundary can be identified on the basis of the diffraction pattern. Repeating the measurement on samples covering the entire composition range completes the phase diagram. These additional samples can be conveniently placed at different locations around the perimeter of the cylindrical rod and rotated into position for diffraction measurement. Temperature-composition phase diagrams for the fully hydrated binary mixtures, dimyristoylphosphatidylcholine (DMPC)/dipalmitoylphosphatidylcholine (DPPC) and dipalmitoylphosphatidylethanolamine (DPPE)/DPPC, have been constructed using the new temperature gradient method. They agree well with and extend the results obtained by other techniques. In the DPPE/DPPC system structural parameters as a function of temperature in the various phases including the subgel phase are reported. The potential limitations of this steady-state method are discussed.

INTRODUCTION

An understanding of lipid–lipid and lipid–water interactions and how these depend on the chemical properties of the lipids requires a knowledge of the conditions governing mesomorphic phase formation. This information is neatly summarized in a temperature-composition phase diagram. A number of different methods have been used to construct phase diagrams of lipid and lipid/water mixtures, including calorimetry, electron microscopy, light scattering, nuclear magnetic and electron spin resonance (ESR), infra-red, fluorescence and Raman spectroscopies, and x-ray and neutron diffraction. Of these, x-ray diffraction is particularly useful because of its ability to identify phases on both sides of a phase boundary and to localize the phase boundary itself. In contrast, other methods can detect the phase boundary but provide little unique information concerning phase identity. Using conventional x-ray sources, phase diagram construction by x-ray diffraction is a laborious and time-consuming process due to low photon flux and consequent lengthy exposure times. With the advent of synchrotron radiation and its greatly enhanced x-ray flux, a large amount of diffraction information can be collected in a relatively short perod of time, allowing phase and structural information to be obtained at significantly increased rates. Seeking to take advantage of this fast data collection, we developed a new method for phase diagram construction using fully hydrated mixtures of dipalmitoylphosphatidylcholine (DPPC) and dipalmitoylphosphatidylethanolamine (DPPE) and mixtures of DPPC and dimyristoylphosphatidylcholine (DMPC). The method makes use of time-resolved x-ray diffraction measurements (Caffrey and Bilderback, 1983, 1984; Caffrey, 1984, 1985) on lipid samples contained in capillaries along which a temperature gradient has been established. The essential features of the method are illustrated in Fig. 1 for a binary lipid mixture. Imposing a temperature gradient along the length of the sample capillary can be viewed as positioning the capillary on a line of constant overall composition (isopleth) in the phase diagram. In this way, the different phases and phase boundaries are localized at different points along the length of the sample capillary. By moving the capillary through the x-ray beam while continuously recording the two-dimensional diffraction pattern, phase changes may be detected by changes in diffraction and the pattern itself serves to identify the phase(s) present at a particular temperature. Repeating the measurement on samples of different composition completes the phase diagram. Because of the temperature gradient, there is no need for repeated temperature changes and sample equilibration, thereby greatly reducing data collection time. That two-dimensional diffraction

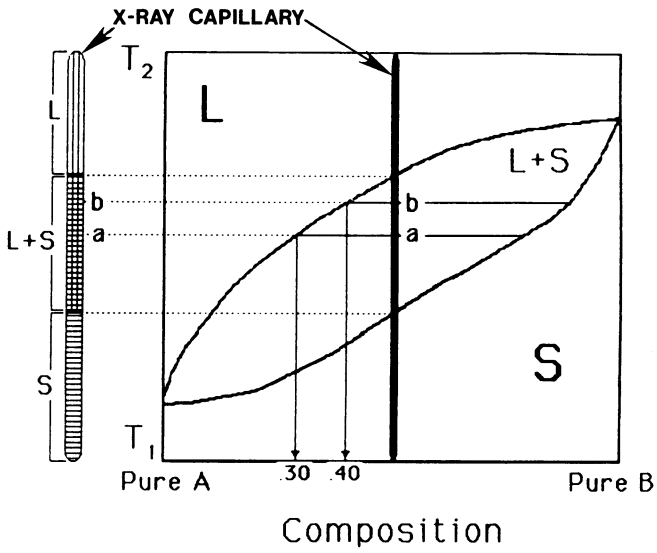

FIGURE 1 Principle of the temperature gradient method for phase diagram construction illustrated using a binary mixture of lipids A and B. The system exhibits a solid or gel (S), a liquid-crystalline phase (L), and a region of phase coexistence (S + L). A capillary containing the lipid or lipid mixture of fixed overall composition is placed on the temperature gradient. Depending on sample composition and the particular gradient imposed, various phases form along the length of the capillary, which are subsequently localized, identified, and quantified by time-resolved x-ray diffraction. The origin of a concentration gradient within the phase coexistence region is accounted for as follows. A temperature gradient from T_1 to T_2 is established along the length of the capillary, which contains a sample whose overall composition is equimolar in lipid A and B. The given phase diagram implies that the composition of the L portion of the sample is 0.4 mol fraction B at point *b* and 0.3 mol fraction B at point *a*. Consequently, there is a decreasing concentration gradient in B from point *b* to point *a* and a gradient of opposite sense for A in the coexistence region.

patterns are recorded also means that problems that might arise by other techniques due to spontaneous sample orientation are obviated in the present method.

The phase properties of fully hydrated mixtures of DMPC and DPPC and of DPPC and DPPE were studied using the temperature-gradient method and compared with results in the literature obtained using a variety of other physical techniques. The two sets are shown to be in excellent agreement. The temperature-gradient data extend our knowledge of the low-temperature region of the DPPC/DPPE phase diagram and provide structural information on the various phases as a function of temperature.

MATERIALS AND METHODS

Materials

L-α-DMPC and L-α-DPPC were purchased from Avanti Polar Lipids, Inc. (Birmingham, AL). L-α-DPPE was obtained from Calbiochem-Behring Corp. (La Jolla, CA). Using 100-μg samples, lipids were judged to be ≥98% pure by thin-layer chromatography in acidic and neutral solvents on two solid supports (K5F silica gel, Whatman Inc., Clifton, NJ; Adsorbosil 5-P plates, Applied Science Laboratories, Waltham, MA) as previously described (Caffrey and Feigenson, 1981). Lipids were used without further purification. All other chemicals and solvents were of reagent grade (Caffrey, 1985).

Sample Preparation

Lipids were dissolved in either $CHCl_3$ (DMPC and DPPC) or a $CHCl_3$/MeOH (9/1, vol/vol) solution (DPPE). To prepare lipid mixtures, appropriate amounts of each lipid in organic solvent were added (30–50 mg total) to a glass test tube and the solvent evaporated under argon gas. Complete solvent removal from the thinly shelled lipid film was accomplished under high vacuum for at least 12 h. The dried lipid was suspended in either Milli-Q purified water (Millipore Corp., Bedford, MA) for DMPC/DPPC mixtures or 100 mM HEPES, pH 7.0 for DPPC/DPPE mixtures, to a final lipid concentration of ~1 mg/ml, by alternately incubating at 70°C and vortexing until a creamy, homogeneous suspension was obtained. Samples were transferred to 1.5-ml centrifuge tubes and spun for 5 min in an Eppendorf centrifuge. Excess clear supernatant was removed and mixtures were pipetted into 1-mm-diam quartz x-ray capillaries (Charles Supper Co., Natick, MA) and spun down at top speed in a clinical centrifuge (Model 1528E; International Equipment Co., Boston, MA). Because of the high viscosity of the hydrated gel phase lipids, some of the mixtures required heating above the gel to liquid-crystal transition temperature during centrifugation to effect pelleting in the capillaries. In preparing some particularly thick mixtures, a number of cycles of pipetting lipid into the sample capillary and centrifuging while heating were required. Capillaries were filled to provide a lipid sample 4 cm long, flame-sealed, and further secured with 5 min epoxy applied to the flame-sealed end. DPPC/DPPE mixtures were stored at 4°C for 3–5 d before taking x-ray measurements. The DPPC/DPPE samples were transferred to the gradient rod from cold storage as quickly as possible (~4 s) to avoid loss of any subgel phase (see below) that might have formed. All samples were incubated on the gradient rod at least 15 min before taking measurements. Thin-layer chromatography (TLC) of samples after diffraction measurements showed ≥98% purity of the lipid.

Temperature Gradient Apparatus

A schematic view of the temperature gradient apparatus is shown in Fig. 2. It consists of a stainless steel cylindrical rod (12 cm long and 1.6 cm in diameter) with a small heater (model 8332; Hotwatt Inc., Danvers, MA) connected to a variable voltage source (The Superior Electric Co., Bristol, CT) positioned in one end. Temperature control at the other end is provided by a circulating water bath. Copper-constantan thermocouples (0.015 in diameter, Omega Engineering Inc., Stamford, CT) are placed along the length of the rod in the positions shown in Fig. 2 to monitor the imposed temperature gradient. Thermocouples were periodically calibrated in an ice/water slush. The sample capillary is placed on top of the rod and secured with Crycon grease to promote good thermal contact. The rod itself is attached to a goniometer head mounted on a computer-controlled, motorized X-Y translation stage. This arrangement provides precise positioning of the sample in the beam. During a scan, horizontal stage position was monitored continuously with a linear potentiometer (model 245103, RVT-S128A, 50Ω, 1163A; Link Aviation Inc., Acton, MA) whose output was recorded and correlated with x-ray beam position along the capillary and with sample temperature. Position along the sample capillary and thus sample temperature are recorded on videotape simultaneously with the x-ray diffraction pattern by directing the linear potentiometer output to a digital voltmeter interfaced with a character generator (serial No. S92, 131–55–11234; Chrono-Log Corp., Havertown, PA). The generator's output is in turn routed to the videotape recorder.

The temperature gradients established on the rod at different water bath and heater (Variac) settings were measured and shown to be approximately linear over the central 5.5-cm length of the rod, and are

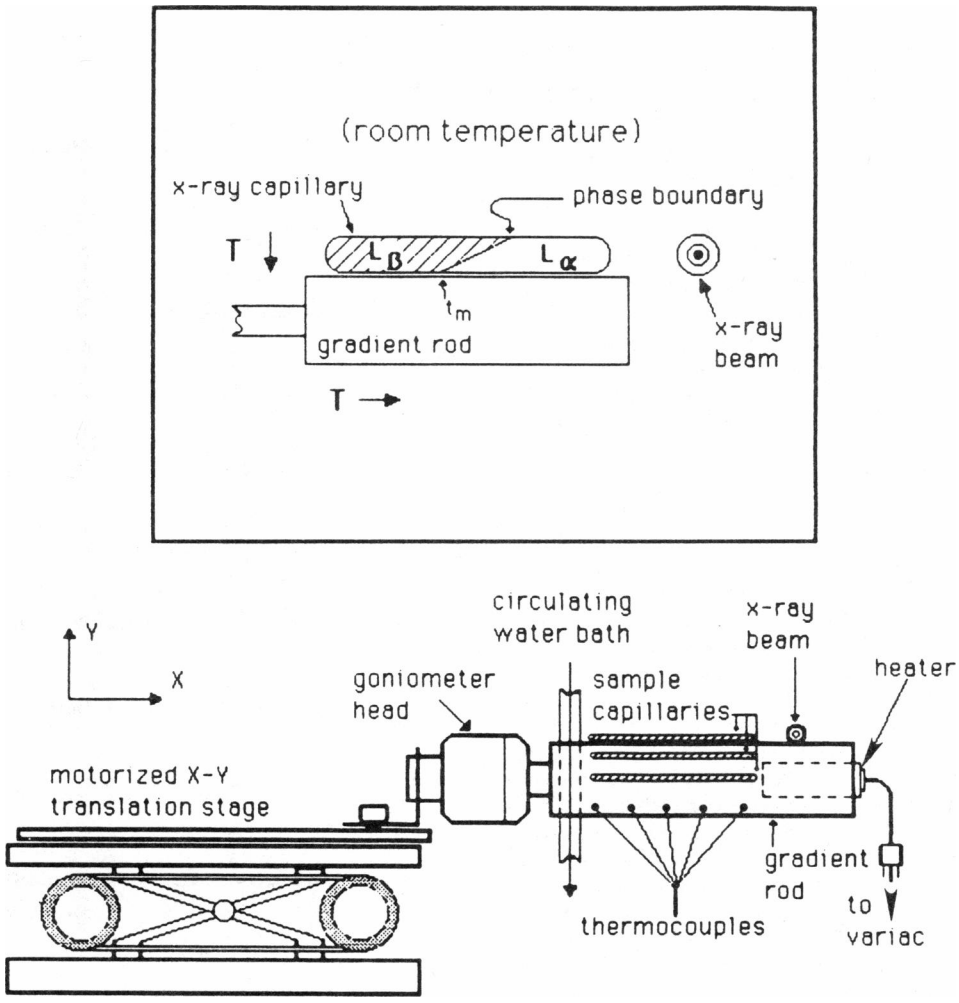

FIGURE 2 Schematic view of the temperature gradient apparatus in the colt revolver arrangement. Temperature controls at the two ends of the rod (heater and water bath) maintain the temperature gradient. Thermocouples monitor temperature along the rod. The eucentric goniometer head allows precise adjustment of the capillaries in the x-ray beam. Horizontal travel of the sample capillary through the beam is provided by the *x-y* translation stage. In the upper portion of this figure the origin of a temperature gradient transverse to the capillary long axis is explained. The capillary shown contains a lipid with L_β and L_α phases with a transition temperature of t_m. At t_m the lipid adjacent to the gradient rod undergoes the transition. Because of the transverse temperature gradient in the capillary and because t_m > room temperature, the phase boundary is shifted toward the right as distance from the rod increases.

remarkably stable. For example, for a 35–90°C gradient, the temperature varied by ±1°C at 86.0°C and ±0.25°C at 40.3°C over a 2-h period.

The thermocouples are secured in holes drilled in the rod and the readings reflect the temperature near the center of the rod. However, the sample capillary sits on the rod surface and to get direct sample temperature readings it is important that there be no significant differences between the internal and external temperatures along the length of the rod. This was confirmed by independent measurements.

X-ray Diffraction

The time-resolved x-ray diffraction method and apparatus has been previously described (Caffrey and Bilderback, 1983, 1984; Caffrey, 1985). Focused, monochromatic radiation at 1.56 Å from the A1 line at the Cornell High Energy Synchrotron Source (CHESS) was used as the x-ray source during which time the Cornell Electron Storage Ring (CESR) was operated at 5.2 GeV and 20–30 mA of electron beam current. All measurements were made with a 0.3-mm-diam collimator (Charles Supper Co.). Diffraction patterns were detected using a modified three-stage image intensifier tube (model 1267-1; Varo Inc., Garland, TX) and a Cohu 500 series TV camera (model 5272-2220/AL4; Cohu Inc., San Diego, CA) and were recorded on a U-Vision NV-9240XD video cassette recorder (Panasonic Co., Secaucus, NJ). Calibration of the intensifier/camera system was accomplished using a standard fully hydrated DPPC multilameller sample at 25°C and using the 64-Å first-order lamellar reflection at low-angles and the 4.2-Å rigid acyl chain reflection at wide-angles.

X-ray capillaries were positioned on top of the gradient rod as shown in Fig. 2 and Crycon grease was used to promote good thermal contact. This grease consists of copper filings in a grease base. The grease has a wide-angle scattering profile similar to that of the "fluid" lipid phase. Throughout these measurements care was taken to ensure that the grease did not contribute to the recorded diffraction patterns.

For accurate d-spacing measurements as a function of temperature, the sample capillary must remain at a fixed sample-to-detector distance as the sample is moved through the x-ray beam. This was assured by proper alignment of the goniometer head and was verified by viewing the capillary through an overhead microscope fitted with eyepiece crosshairs while moving the stage back and forth and by measuring the interlamellar

d-spacing of fully hydrated DPPC at 20°C as a function of position on the rod. The d-spacings vary by ±0.5 Å, indicating a constant sample-to-detector distance along the length (4 cm) of the capillary.

The sample is levelled using the goniometer so that the x-ray beam travels through the middle of the sample capillary, maximizing diffracted intensity and ensuring that diffracted intensity is comparable at all points in the sample. This is complicated, however, by the fact that the capillaries are not of uniform diameter along their length, and by inhomogeneities in the sample (see below).

In certain instances sample length was not sufficient to cover the temperature gradient range of interest. In such cases the sample was progressively moved to higher temperatures on the rod, and measurements were taken so that the entire temperature range could be examined. Failure to make measurements over continuous temperature ranges resulted in missing data in one of the d-spacing plots (Fig. 5).

To maximize resolution low- and wide-angle diffraction regions were examined in separate scans. Diffraction patterns were recorded continuously from the low to the high temperature end of the rod at a rate (depending on the steepness of the gradient) corresponding to ~0.7C°/s.

Data Analysis

The data consist of two-dimensional diffraction patterns from the lipid samples recorded on videotape as a function of time and temperature. Data analysis to determine phase transition temperatures and structural parameters was performed in three ways. First, the temperature gradient scans were viewed directly on a television monitor at both low-angle and wide-angle and any noticeable changes in the diffracted intensity or peak position during the scan were noted. Second, one-dimensional diffracted intensity line scans through the vertical diameter of the diffraction patterns were obtained using an image processor (Grinnell Image Display Buffer, model GMR–274; Grinnell Systems Corp., San Jose, CA) as previously described (Caffrey and Bilderback, 1983). Plotting the data in composite form greatly facilitates detection of changes in intensity and/or peak position (Figs. 3 and 4). Finally, d-spacings for the lipid samples as a function of temperature were calculated from the line scans. A phase transition is indicated in the corresponding d-spacing plot (Fig. 5) by a sudden change in the repeat period with a change in temperature.

RESULTS

DPPC/DPPE Mixtures

The long-spacings of fully hydrated DPPC/DPPE multilamellar mixtures as a function of temperature on a 10–70°C gradient are shown in Fig. 5. Pure DPPC exhibited changes with temperature much like those seen by Janiak et al. (1976) and by Inoko and Mitsui (1978) for the formation by $P_{\beta'}$ phase at 34.5° and 35°C, respectively, using both differential scanning calorimetry (DSC) and x-ray diffraction. A large increase in the d-spacing from 65 to 72 Å occurred at 35°C. In the wide-angle region, the broad shoulder at ~4.06 Å (22°C) on the wide-angle side of the "rigid" acyl chain reflection at 4.2 Å appeared to move inward and become symmetric with the 4.2-Å line; however, this change was more difficult to discern because of interference by the adjacent diffuse water peak (data not shown). Similarly, at 0.1 mol fraction DPPE, formation of the $P_{\beta'}$ phase was seen as a large increase in the d-spacing of the lipid from 67 to 74 Å in the 39.5° to 44°C temperature range accompanied by the same changes in the wide-angle region as was seen in pure DPPC. For mixtures with 0.2 mol fraction DPPE and above, no such increase in the lamellar repeat nor rearrangements in the wide-angle occurred over the temperature range 12° to 70°C.

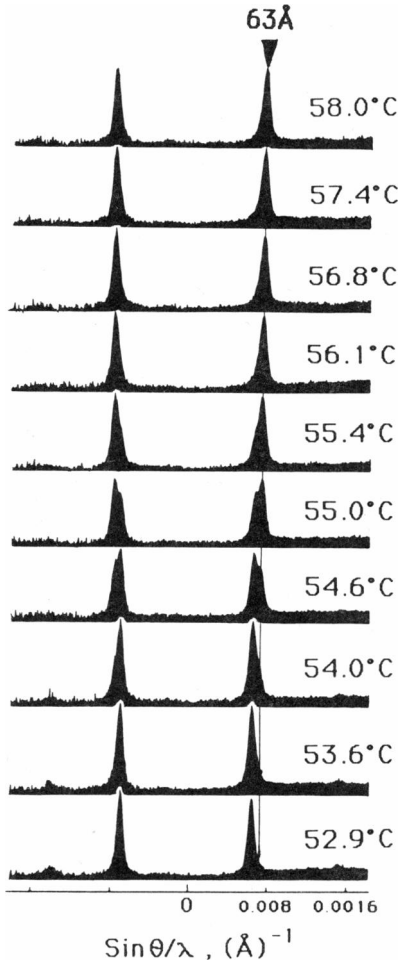

FIGURE 3 Changes in low-angle x-ray diffraction at the order–disorder transition for fully hydrated DPPC/DPPE (0.4/0.6, mol/mol). Diffraction patterns were recorded on videotape and image processed to obtain diffracted intensity profiles as described under Materials and Methods. Each profile represents the average of nine video frames (300 ms at 30 frames/s). Major peaks are due to first-order lamellar reflections. Second-order reflections can be seen at the lower temperatures. The low temperature first-order peak corresponds to a d-spacing of 70 Å.

At DPPE mole fractions of <0.3, evidence for the subgel phase (Chen et al., 1980; Ruocco and Shipley, 1982) at low temperatures was indicated by a smaler lamellar repeat and/or by additional reflections in the diffraction pattern at intermediate angles (Fig. 6). In pure DPPC an increase in d-spacing from 62 to 64 Å occurred from 12° to 16°C, and in the mixture containing 0.1 mol fraction DPPE an increase from 64.8 to 67 Å occurred over a temperature range of 11° to 14°C. Also, an additional peak at ~3.85 Å characteristic of the subgel phase was seen for these two samples, which gradually moved to lower angles and finally merged with the sharp 4.40-Å reflection at higher temperatures. This coincided with the disappearance of the

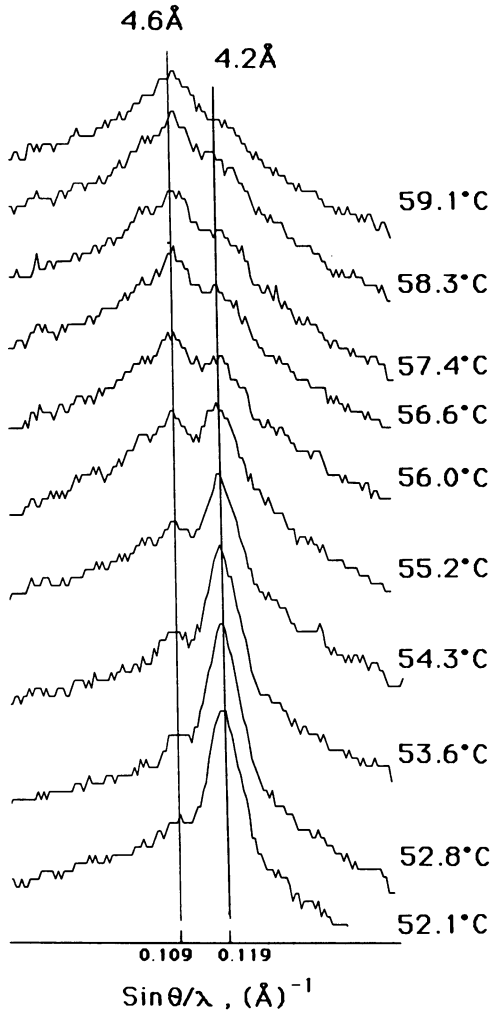

FIGURE 4 Changes in wide-angle x-ray diffraction at the order–disorder transition for fully hydrated DPPC/DPPE (0.4/0.6, mol/mol). For additional details see legend to Fig. 3. Profiles represent the average of 20 video frames (670 ms at 30 frames/s).

intermediate-angle reflection at ~6.7 Å seen at low temperature. For DPPC/DPPE mixtures containing 0.2 and 0.3 mol fraction DPPE, the lamellar repeat at low temperature (<25°C) increased much less, although their rates of increase still appeared discontinuous. An additional peak to the wide-angle side of the 4.4-Å reflection did appear broader and more intense at lower temperatures, and reflections at intermediate angles were noted in the diffraction patterns recorded on videotape, which were absent at higher temperatures (>20°C). These reflections were generally neither as intense nor as well-defined as those seen for pure DPPC and the 0.1 mol fraction DPPE mixture possibly reflecting a less ordered subgel phase in the 0.2 and 0.3 mol fraction DPPE samples. Longer incubations at 4°C may be required to fully develop the subgel phase in these higher DPPE samples. The temperatures at which these intermediate reflections completely disappeared agreed well with the completion of the slight increase in d-spacing seen in the d-spacing plots (Figs. 5 and 7).

Additional reflections at intermediate angles in the diffraction pattern were observed for pure DPPE at low temperatures, suggesting the existence of a subgel phase under these conditions. These reflections faded gradually as temperature increased until ~24°C, when they could no longer be detected and a fully developed lamellar gel phase emerges. There was no corresponding increase in the lamellar repeat over this temperature range, however. This result differs from the observations of Wilkinson and Nagle (1984) who noted in the case of DMPE a direct transition from the subgel to a liquid–crystalline phase without an intermediate L_β phase. The lamellar gel phase of DPPE, therefore, does not appear to be unduly metastable as it was still seen in the 24° to 63°C range after 5 d incubation at 4°C, and there was no increase in the corresponding order–disorder transition temperature (63°C). In lipid mixtures containing between 0.4 and 0.8 mol fraction DPPE, no discontinuity in the rate of increase of the long-spacing at low temperatures was observed nor were there additional reflections at intermediate angles in the diffraction pattern, which might suggest the presence of a subgel phase. These mixtures either do not form this latter phase or they require longer than 3–5 d at 4°C to do so.

The order–disorder transition was apparent in the diffraction patterns as the disappearance of the sharp rigid acyl chain reflection at ~4.2 Å and the emergence of a diffuse band centered at 4.6 Å due to "fluid" acyl chains. In the low-angle region of the diffraction pattern, an additional sharp line became visible to the wide-angle side of the original lamellar reflection as temperature increased through the transition, indicating coexistence of the lamellar gel and liquid-crystalline phases (Caffrey and Bilderback, 1983; Caffrey, 1985). The reflection due to the liquid-crystalline phase gradually increased in intensity and eventually replaced that due to the lamellar gel phase at the higher temperature. These changes are shown in Figs. 3 to 5 for a DPPC/DPPE (0.4/0.6) sample.

The temperatures of the various phase transitions over the entire range of DPPC/DPPE ratios are plotted in Fig. 7 along with the proposed temperature–composition phase diagram. There is some uncertainty as to whether the gel phases (L_β or $L_{\beta'}$, P_β or $P_{\beta'}$) in the mixed lipid range are of the β or β' type since pure DPPC has its acyl chains tilted with respect to the bilayer normal (β') while DPPE does not (β, McIntosh, 1980; Hauser et al., 1981). Because careful static measurements were not performed in the intermediate DPPC/DPPE composition region, a determination of chain tilt angle was not made in the present study. Consequently, the phase fields below the lamellar liquid crystalline and above the subgel phase are designated L_{gel} and P_{gel} in Fig. 7.

DMPC/DPPC Mixtures

The phase diagram for fully hydrated mixtures of DMPC and DPPC multilayers along a temperature-gradient from

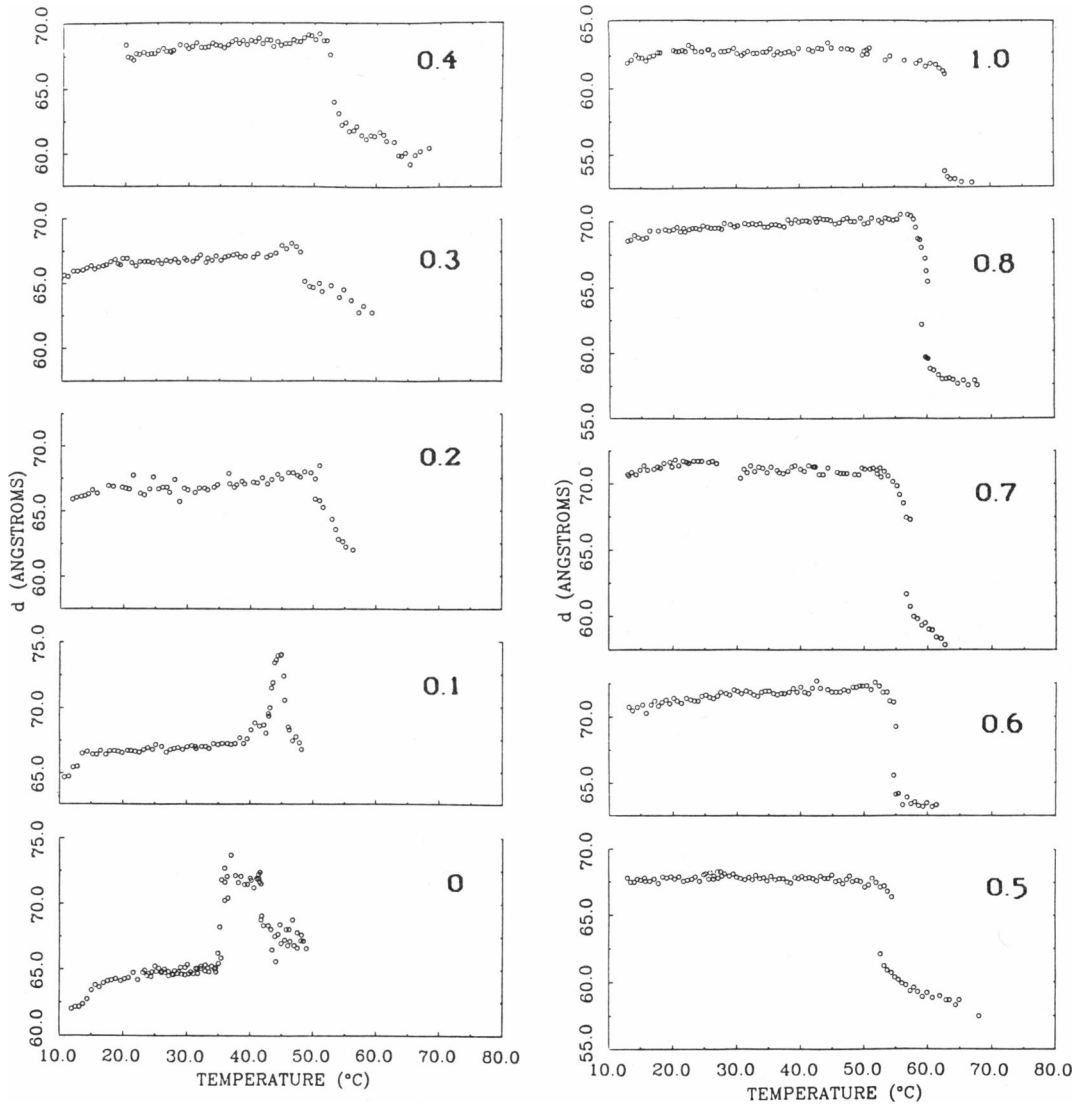

FIGURE 5 Long spacings of fully hydrated DPPC/DPPE mixtures calculated from line scans of first-order lamellar reflections recorded using the time-resolved x-ray diffraction method. The mole fraction DPPE in each mixture is indicated. Due to sample lengths of <4 cm, samples containing 0.7, 0.8, and 1.0 mol fraction DPPE were moved to successively higher temperatures and scanned again until the entire temperature range was covered.

20° to 40°C is shown in Fig. 8. The transition temperatures correspond to onset and completion of the order–disorder transition and were obtained solely from viewing the video recorded wide-angle diffraction patterns as a function of temperature. The changes seen in the diffraction patterns at the various transition temperatures were similar to those described above for mixtures of DPPC and DPPE.

The phase diagram for the DMPC/DPPC system obtained using the temperature-gradient method agrees well with that obtained by other methods (Shimshick and McConnell, 1973; Chapman et al., 1974; Luna and McConnell, 1978). As noted for the DPPC/DPPE system (see below), the region of coexistence obtained using the temperature-gradient method is generally narrower than that obtained by other methods although it still falls within the same temperature range for a given composition.

DISCUSSION

The temperature gradient method has been used to construct temperature-composition phase diagrams for fully hydrated DPPC/DPPE and DPPC/DMPC multilamellar mixtures. In both instances our findings agree with and extend data obtained by a variety of other methods. A phase diagram for DPPC/DPPE in excess water has been proposed by Blume et al. (1982 and references therein) based on ^{13}C and ^{2}H-NMR studies and on data from ESR, DSC, chlorophyll *a* fluorescence, and Raman spectroscopy. The phase coexistence regions as determined by the present temperature gradient method are generally narrower than those reported for other methods. This may be due to a lower sensitivity of x-ray diffraction to subtle changes in molecular arrangements (Melchior and Steim,

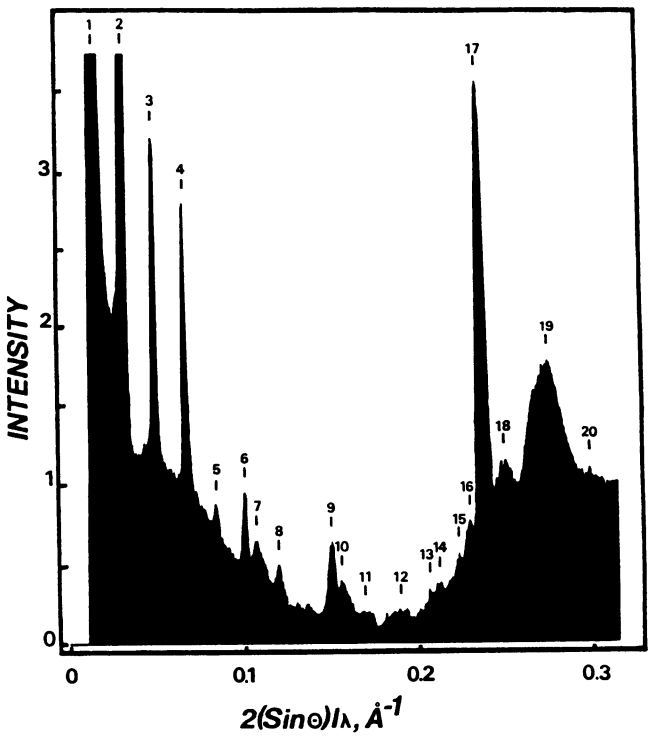

FIGURE 6 Microdensitometric scan of an x-ray photograph of the subgel phase in fully hydrated DPPC multilamellar vesicles. Samples were incubated at 0–4°C for 13 d before measurement at 8°C in a 1-mm quartz capillary using a 0.3-mm collimator. Exposure time was 15 min at 5.24 GeV, 15 mA. The d-spacings of the peaks indicated are as follows: 1, 5.89; 2, 2.95; 3, 1.96; 4, 1.47; 5, 1.19; 6, 0.990; 7, 0.930; 8, 0.824; 9, 0.668; 10, 0.646; 11, 0.601; 12, 0.540; 13, 0.495; 14, 0.485, 15, 0.460; 16, 0.451; 17, 0.440; 18, 0.418; 19, 0.385 and 20, 0.355 nm. The scan was made using a microdensitometer (model 111c; Joyce-Loebl, Gateshead, England.)

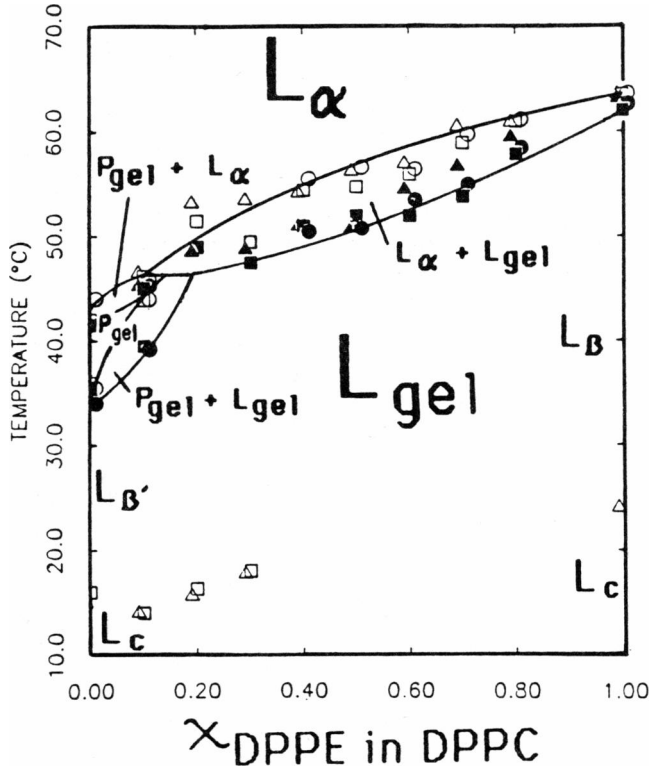

FIGURE 7 Proposed phase diagram for the DPPC/DPPE multilamellar system in excess aqueous phase. Onset and completion phase transition temperatures were determined by three different types of observations of diffraction data: (*open circle*) d-spacing plots; (*open square*) visual inspection of low-angle diffraction data on a video monitor; (*open triangle*) visual inspection of wide-angle diffraction data on a video monitor. Solid and open symbols denote, respectively, onset and completion transitions in the direction of increasing temperature. Estimated error in temperature is ±1.5°C. It is emphasized that along each isopleth phase determination has been made continuously over the full temperature range indicated and that for sake of clarity only the phase boundaries are shown.

1979). It may also indicate that the transitions themselves are intrinsically more sharp and that the temperature gradient method accurately reflects this. In the current work, the P_{gel} phase was seen at <0.2 mol fraction DPPE as opposed to concentrations of up to 0.5 mol fraction DPPE observed by Blume et al. (1982). This difference is partially attributable to the different techniques used inasmuch as the temperature gradient method is not an equilibrium method (see below). The phase diagram proposed in Fig. 7 is similar to that described by Luna and McConnell (1978) for fully hydrated DPPE/DMPC mixtures in having three two-phase regions which meet at a three-phase line located, in the present case, at 46°C.

Transition temperatures determined from d-spacing plots (Fig. 5) and from visual inspection of diffraction patterns recorded on videotape compared well (±1°C) with each other. Further, the low-angle diffraction data were more sensitive to the start of the order–disorder transition than the wide-angle data, since the appearance of a sharp reflection at low-angles was easier to detect than an increase in diffuse scatter at wide angles (Caffrey and Feigenson, 1984). However, the sensitivity for detecting completion of the transition was better at wide angles. This

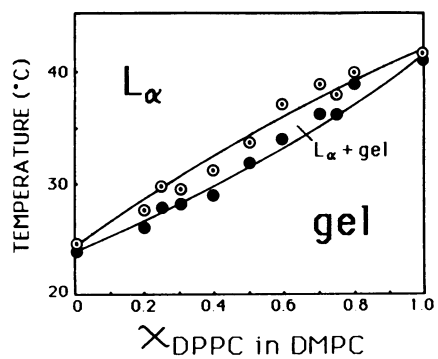

FIGURE 8 Phase diagram of fully hydrated DMPC/DPPC multilamellar mixtures. Phase transition temperatures were obtained based on wide-angle x-ray diffraction data recorded using the temperature gradient method as described in the text. The low temperature phase is designated "gel" since an independent determination of its lattice type and symmetry was not made in these experiments. Phase boundaries are included in the diagram for clarity only.

is reflected in Fig. 7 by the lower onset temperatures using low-angle data and the higher completion temperatures using wide-angle information.

As an independent check on the validity and internal consistency of the phase diagram obtained using the temperature gradient method, we verify the following prediction. The structural parameters observed for the L_α and L_{gel} phases in the coexistence region of Fig. 7 should be those of the corresponding solidus and fluidus compositions at a given temperature and overall lipid composition. The data in Fig. 7 indicate a fluid and gel phase composition (X_{DPPE}) of 0.4 and 0.7, respectively, at 55°C and an overall lipid composition of 0.6. Referring to Fig. 5 we see that at 55°C samples of composition 0.4 and 0.7 have interlamellar d-spacing values of 62.5 and 70 Å, respectively. These are in excellent agreement with the structural parameters of 63 and 70 Å observed in the coexistence region as reported in Fig. 3.

At this juncture the advantages and disadvantages of the temperature gradient method and its use in temperature-composition lipid phase diagram construction will be considered. To begin with, the method is intuitively simple (Fig. 1): samples contained in long capillaries arranged around the perimeter of a rod upon which a temperature gradient has been imposed represent isopleths (lines of constant overall composition) in the phase diagram. The time-resolved x-ray diffraction method facilitates rapid phase identification and quantitation in temperature-composition space.

The fact that x-ray diffraction is used to provide phase information offers many advantages. It gives positive phase identification both in single and multiple phase regions and allows us to locate phase boundaries. From the diffraction data itself structural parameters of the various phases can be obtained along each isopleth continuously as a function of temperature. The continuous nature of the method is also important because it means that phase fields or coexistence regions that exist over narrow temperature regions will be readily detected. Because the method is quantitative, the relative amounts of phases in phase coexistence regions can be determined (see Caffrey, 1985). This can be used to great advantage in verifying interpolated phase boundaries in the phase diagram.

The use of diffraction for phase identification and quantitation also means that artifacts, which might arise with other methods due to preferential sample orientation, especially in one-phase regions, are avoided. We emphasize, however, that this relies on the use of a two-dimensional detector. The diffraction method also obviates the need for additives or molecular labels, both of which are potentially perturbing. An added convenience of the present system is that data is recorded on videotape. The data can, therefore, be carefully reviewed at leisure in replay mode at selected speeds and the appropriate segments identified for subsequent image processing.

While x-rays at the intensity available through synchrotron radiation can be damaging (Caffrey, 1984), the temperature gradient method requires that a particular portion of the sample is in the beam for a very short period of time. Thus, the method is nondestructive and the sample can be recovered for reuse. This offsets one of the disadvantages of the method, namely the need for large amounts of material. For example, to prepare a fully hydrated DPPC sample 1 mm in diameter and 4 cm long requires 30–50 mg lipid.

The main advantage of the method is data acquisition speed. No longer is it necessary to equilibrate samples at each successive temperature before making the diffraction measurements. With samples of different compositions positioned lengthwise around the perimeter of the cylinder in a colt revolver fashion (Fig. 2) all that is required is to allow the samples to reach a steady-state on the gradient and to make the diffraction measurements. This takes on the order of 30–60 s/sample. In principle, the data for a complete phase diagram with 15–20 isopleths could be collected by this method in 1 h of beam time. The ability to collect data quickly also means that systematic and nonsystematic errors due to sample source and preparation, and to data acquisition and analysis procedures are minimized.

Finally, the temperature gradient method offers the advantage of scale expansion or contraction. For example, if the intention is to obtain information on the general phase behavior of a system over a wide temperature range, the temperature gradient can be so set up. This should be extremely useful in survey type work. If, on the other hand, the intent is to investigate a particularly narrow phase coexistence or transition region, the temperature gradient can be very conveniently expanded in the region of interest for detailed examination. In this context we note that it is not necessary to limit oneself to linear temperature gradients. Gradients of different profiles are available by an appropriate choice of gradient rod shape (Holman, 1976).

On the negative side, the temperature gradient method is dependent on having access to items of high technology. These include a monochromatic x-ray beam of high intensity of the type that is available at a synchrotron source, a two-dimensional x-ray imaging device, video equipment and, for quantitative data analysis, image processing capabilities. Of course, detection, recording, and analysis systems other than the ones described above are possible and in certain instances may be even more desirable. The point is that a complete system in one form or another should be available at each of the synchrotron radiation facilities around the world (Winick, 1980).

Sample homogeneity is a potential problem. Trapped air bubbles give rise to missing data points in diffracted intensity scans and must be eliminated by careful centrifugation and possibly the use of degassed solvent. Centrifugation itself can generate sample concentration gradients

along the length of the capillary. While not a big problem, it does lead to gradual changes in diffracted intensity from one end of the sample to the other.

A rate-limiting step in this procedure is alignment of capillaries, particularly when operating with the colt revolver arrangement shown in Fig. 1. The only way around this is to have available an arsenal of gradient rods mounted on goniometer heads upon which capillaries have been aligned ahead of time. This will ensure the most efficient use of beam time.

No insulation is provided in the present experimental arrangement, and a temperature gradient exists transverse to the long-axis of the capillary (Fig. 2). This arises because only one side of the capillary contacts the gradient rod while the other side is exposed to air at ambient temperatures. The net result is to slightly broaden and to shift transition temperatures since the x-ray beam now samples a diagonal rather than a vertical phase boundary. Enclosing the apparatus in a vacuum chamber will eliminate this problem. We note, however, that in the temperature range examined in the present set of experiments this effect was minimal in terms of measured transition temperatures.

Finally, the issue that the temperature gradient method is a steady-state rather than an equilibrium technique must be addressed, particularly since the intent is to use it in constructing phase diagrams that are for the most part considered to reflect a true equilibrium and to follow the Gibbs phase rule. While it is true that the method is steady-state, the empirical observation is that it works. Phase diagrams obtained by this method are in excellent agreement with those obtained by other more standard "equilibrium" methods. At least in the cases examined, therefore, the steady-state issue does not appear to be a problem. However, it is instructive to examine the situation that prevails, for example, in a two-phase coexistence region upon which a temperature gradient is imposed. To this end, let us consider the phase diagram shown in Fig. 1. We note that in the phase coexistence region a concentration gradient of the two component lipid species (A and B) exists along the length of the capillary. For the moment we will address the situation in the liquid-crystalline fraction since, by comparison, molecular diffusion in the gel phase is extremely slow (Alecio et al., 1982). Referring to Fig. 1, we see that the liquid-crystalline phase is $0.7A$ and $0.3B$ at position a in a sample whose overall composition is equimolar in A and B. However, at the higher temperature represented by point b in the capillary, the composition is $0.6A$ and $0.4B$. Thus, for lipid A a concentration gradient exists from b to a whereas for lipid B the gradient is in the opposite direction. By extension a concentration gradient exists for both lipids at all points in the phase coexistence region, which should drive lipid diffusion.

To determine if this effect brought about any noticeable change in the phase diagram measurements were carried out on an equimolar mixture of DPPC and DMPC incubated on the gradient rod for 15 min and for 2 h. In both cases the onset and completion transition temperatures were the same to within experimental error and agreed well with those obtained by DSC (Chapman et al., 1974). It appears, therefore, that lipid diffusion is inconsequential on the time-scale of these experiments. Perhaps it is because lipids are confined to individual multilamellar vesicles between which lipid exchange is slow (Schroit and Madsen, 1983; Tamura et al., 1986) that accounts, at least in part, for this result. Diffusion is more likely to be a problem in systems that exhibit phase coexistence, one phase of which is an isotropic fluid.

CONCLUSION

A new "steady-state" method is described that combines time-resolved x-ray diffraction and a temperature gradient for temperature-composition lipid phase diagram construction at unprecedented rates. The method has been used to construct phase diagrams for fully hydrated DPPC/DPPE and for DPPC/DMPC multilamellar mixtures, which agree with and extend data obtained by a variety of other physical techniques. Advantages of the new method include rapid data acquisition rates and sample throughput, positive phase identification and quantitation, and structural parameter determination continuously with temperature in single and multiple phase regions. The method is also inexpensive, nonperturbing, nondestructive, insensitive to orientation effects, and offers the ability to change the temperature gradient range and profile at will. Further, the two-dimensional data recorded on videotape can be examined at leisure in replay mode. The method does, however, require access to a high intensity, monochromatic x-ray source and to suitable detection, recording, and analysis devices, relatively large amounts of sample, and careful sample alignment. It would be greatly improved by the provision of an evacuated sample chamber and by a guarantee of sample homogeneity.

The authors thank B. W. Batterman (National Science Foundation grant DMR81-12822), D. H. Bilderback, G. W. Feigenson (National Institutes of Health grant HL-18255), and J. K. Moffat (National Institutes of Health grants RR-01646 and GM29044) for their invaluable help and support. Further thanks go to W. W. Webb for making available the Grinnell image processing system and to Ellen Patterson for carefully typing the manuscript.

This work incorporates the undergraduate senior thesis of F. S. Hing and was supported in part by a Grant-in-Aid of Research from Sigma Xi, the Scientific Research Society, and The National Institutes of Health, grant number DK36849, to M. Caffrey.

Received for publication 12 May 1986 and in final form 4 September 1986.

REFERENCES

Alecio, M. R., D. E. Golan, W. R. Veatch, and R. R. Rando. 1982. Use of a fluorescent cholesterol derivative to measure lateral mobility of

cholesterol in membranes. *Proc. Natl. Acad. Sci. USA.* 79:5171–5174.

Blume, A., R. J. Wittebort, S. K. Das Gupta, and R. G. Griffin. 1982. Phase equilibria, molecular conformation, and dynamics in phosphatidylcholine/phosphatidylethanolamine bilayers. *Biochemistry.* 21:6243–6253.

Caffrey, M. 1984. X-radiation damage of hydrated lecithin membranes detected by real-time x-ray diffraction using wiggler-enhanced synchrotron radiation as the ionizing radiation source. *Nucl. Instrum. and Meth.* 222:329–338.

Caffrey, M. 1985. Kinetics and mechanism of the lamellar gel/lamellar liquid-crystal and lamellar/inverted hexagonal phase transition in phosphatidylethanolamine: a real-time x-ray diffraction study using synchrotron radiation. *Biochemistry.* 24:4826–4844.

Caffrey, M., and D. H. Bilderback. 1983. Real-time x-ray diffraction using synchrotron radiation: system characterization and applications. *Nucl. Instrum. and Meth.* 208:495–510.

Caffrey, M., and D. H. Bilderback. 1984. Kinetics of the main phase transition of hydrated lecithin monitored by real-time x-ray diffraction. *Biophys. J.* 627–631.

Caffrey, M., and G. W. Feigenson. 1981. Fluorescence quenching in model membranes: relationship between calcium adenosinetriphosphatase enzyme activity and the affinity of the protein for phosphatidylcholines with different acyl chain characteristics. *Biochemistry.* 20:1949–1961.

Caffrey, M., and G. W. Feigenson. 1984. Influence of metal ions on the phase properties of phosphatidic acid in combination with natural and synthetic phosphatidylcholines: an x-ray diffraction study using synchrotron radiation. *Biochemistry.* 23:323–331.

Chapman, D., J. Urbina, and K. M. Keough. 1974. Biomembrane phase transitions. Studies of lipid-water systems using differential scanning calorimetry. *J. Biol. Chem.* 249:2512–2521.

Chen, S. C., J. M. Sturtevant, and B. J. Gaffney. 1980. *Proc. Natl. Acad. Sci. USA.* 77:5060–5063.

Hauser, H., I. Pascher, R. H. Pearson, and S. Sundell. 1981. Preferred conformation and molecular packing of phosphatidylethanolamine and phosphatidylcholine. *Biochim. Biophys. Acta.* 650:21–51.

Holman, J. P. 1976. Heat Transfer, 4th ed. McGraw-Hill Inc., New York.

Inoko, Y., and T. Mitsui. 1978. Structural parameters of dipalmitoylphosphatidylcholine lamellar phases and bilayer phase transitions. *J. Phys. Soc. Jpn.* 44:1918–1924.

Janiak, M. J., D. M. Small, and G. G. Shipley. 1976. Nature of the thermal pretransition of synthetic phospholipids: dimyristoyl- and dipalmitoyllecithin. *Biochemistry.* 15:4575–4580.

Luna, E. J., and H. M. McConnell. 1978. Multiple phase equilibria in binary mixtures of phospholipids. *Biochim. Biophys. Acta.* 509:462–473.

McIntosh, T. J. 1980. Differences in hydrocarbon chain tilt between hydrated phosphatidylethanolamine and phosphatidylcholine bilayers: a molecular packing model. *Biophys. J.* 29:237–246.

Melchior, D. L., and J. M. Steim. 1979. Lipid-associated thermal events in biomembranes. *Prog. Surf. Membr. Sci.* 13:211–290.

Ruocco, M. J., and G. G. Shipley. 1982. Characterization of the subtransition of hydrated dipalmitoylphosphatidylcholine bilayers. X-ray diffraction study. *Biochim. Biophys. Acta.* 684:59–66.

Schroit, A. J., and J. W. Madsen. 1983. Synthesis and properties of radioiodinated phospholipid analogues that spontaneously undergo vesicle-vesicle and vesicle-cell transfer. *Biochemistry.* 22:3617–3623.

Shimshick, E. J., and H. M. McConnell. 1973. Lateral phase separation in phospholipid membranes. *Biochemistry.* 12:2351–2360.

Tamura, A., K. Yoshikawa, T. Fujii, K. Ohki, Y. Nozawa, and Y. Sumida. 1986. Effect of fatty acyl chain length of PC on their transfer from liposomes to erythrocytes and transverse diffusion in the membranes inferred by TEMPO-PC spin probes. *Biochim. Biophys. Acta.* 855:250–256.

Wilkinson, D. A., and J. F. Nagle. 1984. Metastability in the phase behavior of dimyristoylphosphatidylethanolamine bilayers. *Biochemistry.* 23:1538–1541.

Winick, H. 1980. Synchrotron radiation sources, research facilities, and instrumentation. *In* Synchrotron Radiation Research. H. Winick, and S. Doniach, editors. Plenum Publishing Corp., New York. 27–60.